

# Downlink Coverage and Rate Analysis of an Aerial User in Integrated Aerial and Terrestrial Networks

Nesrine Cherif\*, Mohamed Alzenad<sup>†</sup>, Halim Yanikomeroglu<sup>†</sup>, and Abbas Yongacoglu\*.

\*School of Electrical Engineering and Computer Science, University of Ottawa, Ottawa, ON, Canada.

<sup>†</sup> Department of Systems and Computer Engineering, Carleton University, Ottawa, ON, Canada.

Email: \*{ncher082, yongac}@uottawa.ca, <sup>†</sup>{mohamed.alzenad, halim}@sce.carleton.ca.

**Abstract**—In this paper, the downlink coverage probability and average achievable rate of an aerial user in a vertical HetNet (VHetNet) comprising aerial base stations (aerial-BSs) and terrestrial-BSs are analyzed. The locations of terrestrial-BSs are modeled as an infinite 2-D Poisson point process (PPP) while the locations of aerial-BSs are modeled as a finite 3-D Binomial point process (BPP) deployed at a particular height. We adopt cellular-to-air (C2A) channel model that incorporates LoS and NLoS transmissions between the terrestrial-BSs and the typical aerial user while we assume LoS transmissions for the air-to-air (A2A) channels separating the aerial user and aerial-BSs. For tractability reasons, we simplify the expression of the LoS probability provided by the International Telecommunications Union using curve fitting. We assume that the aerial user is associated with the BS (either an aerial-BS or terrestrial-BS) that provides the strongest average received power. Using tools from stochastic geometry, we derive analytical expressions of the coverage probability and achievable rate in terms of the Laplace transform of interference power. To simplify the derived analytical expressions, we assume that the C2A links are in LoS conditions. Although this approximation gives pessimistic results compared to the exact performance, the analytical approximations are easier to evaluate and quantify well the performance at high heights of the aerial user. Our findings reveal that using directive beamforming for the aerial-BSs improves the downlink performance substantially since it alleviates the strong interference signals received from the aerial-BSs.

**Index Terms**—Aerial-BS, coverage probability, stochastic geometry, Poisson point process, Binomial point process.

## I. INTRODUCTION

Unmanned aerial vehicles (UAVs, also referred to as drones) are being introduced as a flexible solution in future wireless networks to improve their performance and flexibility [1], [2]. For instance, a drone (also referred to as an aerial user) can be deployed in the case of a natural disaster to complete a rescue mission in hard-to-reach areas [3]. Moreover, aerial users can be seen as the next generation for package delivery purposes. In fact, Amazon started its prime air delivery that promises to deliver packages to customers from the sky [4], [5]. The promising applications where aerial users can be deployed are diverse, thanks to their flexible deployment and extended degrees of freedom, that make them more effective in performing different tasks and delivering services in a quick manner in comparison to traditional ways. A UAV can also be

equipped with a BS that can provide wireless connectivity to users (terrestrial and/or aerial users) [6]. Indeed, aerial-BSs have been proposed confidently as an agile and a quick-to-deploy network entity in the case of emergency situations and/or high capacity demands (e.g., during a temporary event) [7]–[9]. In addition, aerial-BSs have been introduced as a solution that can provide ubiquitous wireless connectivity to remote communities around the world where the deployment of fixed terrestrial-BSs deemed challenging [10].

Despite the fact that the coexistence of aerial and terrestrial networks, which is referred to as the vertical HetNet (VHetNet) [11], along with aerial users will be so prominent in the near future, the performance of such networks for the aerial users in terms of the downlink coverage and achievable rate has not been studied yet. The non-homogeneity between aerial and terrestrial networks can be seen from different perspectives: (1) the terrestrial network can be seen as an infinite network, the aerial network, however, consists of a finite number of aerial-BSs, (2) while the terrestrial network is in 2-D, its aerial counterpart is in 3-D which adds more differences in the characteristics of each architecture.

### A. Related Work

Due to the emerging applications of UAVs as aerial-BSs and aerial users (e.g., delivery-drones), the performance of the VHetNets that involve aerial users as well as terrestrial users received a great interest. The authors in [12] and [13] investigate the feasibility of serving aerial and terrestrial users using a terrestrial wireless network. The authors claim that the LoS conditions that the aerial users experience with the terrestrial-BSs degrade the SINR at the terrestrial users due to the strong interference signals received from the LoS aerial users. Furthermore, the work in [12] and [13] present several tuning parameters to combat these strong interference signals. However, they do not consider the existence of aerial-BSs which could be a candidate to serve aerial users, especially if the terrestrial wireless network is congested. The downlink coverage of a typical terrestrial user served by a network of finite aerial-BSs is studied in [14]. In this work, the links between the terrestrial users and aerial-BSs are assumed to be in LoS conditions (NLoS links are not considered). Such assumption may not be applicable to aerial-BSs that operate at very low heights and/or in dense environments due to the high likelihood of the NLoS occurrence in these scenarios.

This work was supported in part by the Ministry of Higher Education and Scientific Research, Libya, through the Libyan-North American Scholarship Program, and in part by Huawei Canada Co. Ltd.

In addition, the work in [14] limits the association of the terrestrial user to only aerial-BSs, and do not consider the fact that the terrestrial user might be served by a nearby terrestrial-BS that provides a better channel condition than that provided by an aerial-BS if it exists. Similar to the work presented in [12], the authors in [15] investigate the opportunity of re-utilizing the existing terrestrial wireless networks in serving aerial users. The work suggests several interference mitigation techniques both in the uplink and downlink transmissions in order to maintain an acceptable performance of the terrestrial network towards both terrestrial and aerial users. Utilizing coordinated multi-point transmissions to provide a seamless cellular connectivity to aerial users is studied in [16]. Clustered small cell BSs are considered for serving aerial users in content-caching architecture where a requested popular content is cached to aerial users which could be transmitted to terrestrial users from the sky. However, the work in [16] is only limited to the scenarios where terrestrial-BSs do not coexist with aerial-BSs. The authors in [11] propose a framework to analyze the coverage and rate of the VHetNet. However, the analysis, in this work, is done for a typical terrestrial user, and hence it is not applicable for aerial users.

### B. Contributions

We propose a framework to analyze the downlink coverage and rate of an aerial user served by a VHetNet comprising aerial-BSs and terrestrial-BSs. The model consists of terrestrial-BSs that follow an infinite 2-D PPP and aerial-BSs that follow a finite 2-D BPP deployed at a particular height above the ground [14]. We model the C2A links according to the general framework provided by the International Telecommunications Union (ITU) in its recommendation report [17] that incorporates LoS and NLoS transmissions occurring according to a given probability. However, the expression of the LoS probability is analytically intractable and difficult to use. The widely used air-to-ground (A2G) channel model proposed in [18], [19], which is based on the ITU-recommendation report [17], is developed for terrestrial users and is thus not applicable to the C2A channels for the aerial users. To the best of our knowledge, there is no simple and analytically tractable expression for the probability of LoS occurrence based on the ITU recommendation report [17]. Therefore, we use curve fitting to approximate the LoS probability expression, and we show that the approximated LoS probability matches closely that of the ITU model in [17]. On the other hand, the A2A are assumed to be in LoS conditions due to the absence of obstacles between the aerial user and aerial-BSs. In order to alleviate the strong interference signals received from the aerial-BSs, we incorporate directional beamforming at the aerial-BSs, where the aerial-BS beam is directed towards the typical aerial user with a certain probability. Two spectrum sharing policies between aerial-BSs and terrestrial-BSs (referred to as orthogonal spectrum sharing (OSS) and non-OSS (N-OSS)) are considered.

We derive analytical expressions for the coverage probability and rate in terms of the Laplace transform of interference power, and we show that the derived expressions match the

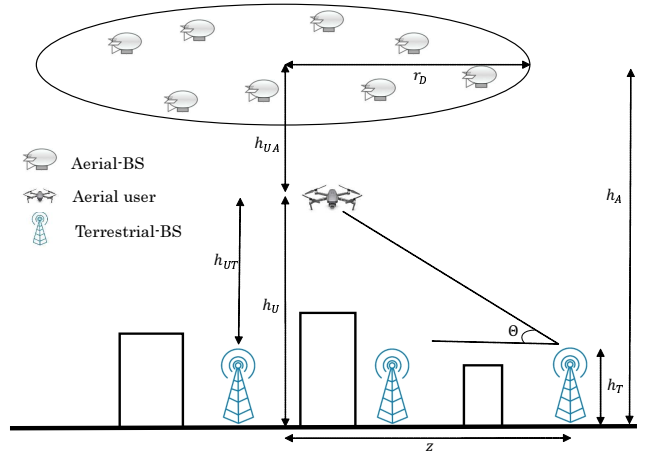


Fig. 1. Terrestrial and aerial VHetNet.

simulations. To simplify the analysis, we further assume that the C2A links are all in LoS conditions (no NLoS transmissions). Under this assumption, closed-form expressions for the association probabilities and the Laplace transform of the terrestrial interference power are derived. The analytical analysis of the interference received from the aerial-BSs is challenging, especially because of the beamforming that directs the main beam of the aerial-BS towards the typical aerial user with a certain probability. This assumption results in two dependent tiers of aerial-BSs where the number of aerial-BSs in each tier depends on the other. Based on this setup, we derive an exact expression for the Laplace transform of the interference received from aerial-BSs in terms of Meijer-G function. To the best of our knowledge, none of the existing works present a closed-form expression for the interference received from aerial-BSs. In fact, it is often presented as an integral expression. This derived closed-form expression simplifies the evaluation of the expressions of the coverage probability and rate. Furthermore, assuming that all the C2A channels are in LoS conditions results in deriving closed-form expression for the Laplace transform of the interference received from terrestrial-BS in terms of the Meijer-G function.

This paper is organized as follows. The system model is presented in Section II. In Section III, we derive expressions for the association probabilities and the Laplace transforms of the aggregated interference powers. Furthermore, we derive some useful distance distributions which will be used in the subsequent sections. Closed-form expressions for the coverage probability and the average achievable rate are derived in Section IV. Finally, we validate and compare the derived analytical expressions with Monte Carlo simulations, and investigate the impact of several system parameters on the performance of the VHetNet.

## II. SYSTEM MODEL

We assume a network of single tier terrestrial-BSs, denoted by  $\Phi_T$ , uniformly distributed on the ground (i.e., terrestrial-BSs follow PPP) with density  $\lambda_T$  [terrestrial-BSs/km<sup>2</sup>] and

height  $h_T$ <sup>1</sup>. We assume a network of  $N$  aerial-BSs hovering at a height  $h_A$  from the ground and uniformly distributed over a disc (i.e., aerial-BSs follow a BPP) with a center  $(0, 0, h_A)$  and radius  $r_D$ . It is worth mentioning that the performance of a network of aerial-BSs deployed uniformly at different heights in the range  $[h_{\min}, h_{\max}]$  matches perfectly that of aerial-BSs deployed at the same height given by  $\frac{h_{\min}+h_{\max}}{2}$  [14]. Therefore, although we place the aerial-BSs at the same height  $h_A$ , our framework is still applicable for aerial-BSs with different heights. The transmit power of the terrestrial-BSs and aerial-BSs are assumed to be  $P_T$  and  $P_A$ , respectively. We consider a typical aerial user hovering at a height  $h_U$  where  $h_T < h_U < h_A$ .

#### A. Cellular-to-air channel

The widely used A2G channel model proposed in [18], [19] is not applicable to aerial users because it is developed for terrestrial users with heights of 1.5 meters while our system model involves terrestrial-BSs with much larger heights (e.g., 30 meters for macro-BSs) [20]. Therefore, in this section, we develop a more tractable expression for the LoS probability. According to the ITU recommendation report [17], the probability of LoS between a transmitter and a receiver of heights  $h_{TX}$  and  $h_{RX}$ , respectively, is given by [17]

$$P_L(z) = \prod_{n=0}^m \left[ 1 - \exp \left( - \frac{\left[ h_{TX} - \frac{(n+\frac{1}{2})(h_{TX}-h_{RX})}{m+1} \right]^2}{2\delta^2} \right) \right], \quad (1)$$

where  $z$  denotes the horizontal distance between the transmitter and the receiver in the  $xy$  plane, and  $m = \lfloor \left( \frac{z\sqrt{\alpha\beta}}{1000} - 1 \right) \rfloor$  where  $\alpha$ ,  $\beta$ , and  $\delta$  are environment-related coefficients given in Table I in [21].

As can be easily seen from (1), the LoS probability  $P_L(z)$  is not a continuous function of  $z$  which makes the analytical analysis intractable. Similar to the work in [18], [19], we simplify (1) to a more tractable Sigmoid function under some assumptions. This can be done by approximating the curve of  $P_L(z)$  in (1) by a continuous exponential function of the elevation angle  $\theta$  for a fixed terrestrial-BS height. From Fig.1, the horizontal distance  $z$  can be written as  $z = (h_U - h_T) / \tan(\theta)$ . Comparing the parameters in (1) with the parameters of the system model presented in Fig.1, we have,  $h_{TX} = h_T$  and  $h_{RX} = h_U$ . Using the Matlab<sup>®</sup> feature 'Curve Fitting', we have

$$P_L(\theta) = -a \exp(-b\theta) + c, \quad (2)$$

where  $\theta = \tan^{-1} \left( \frac{h_U - h_T}{z} \right)$ , and  $a$ ,  $b$ , and  $c$  are parameters that depend on the environment and the height of the terrestrial-BSs. It is worth mentioning that the discrete expression of  $P_L(z)$  in (1) smooths at very large aerial user heights which yields a continuous function of  $\theta$  that can be easily fitted to a more simple equation. We summarize the LoS probability model used in this paper in table I.

<sup>1</sup>Although terrestrial-BSs are often a mix of macro-, micro-, or pico-BSs, we only consider a single tier terrestrial network composed of macro-BS since macro-BSs transmit at higher powers than other terrestrial-BSs and are thus more suitable for providing wireless connectivity to aerial users.

TABLE I  
APPROXIMATED LOS PROBABILITIES FOR DIFFERENT ENVIRONMENTS

Environment	$h_T$ (meters)	a	b	c
Suburban	30	1	6.581	1
Urban	19	1	0.151	1
Dense urban	25	1	0.106	1
Highrise urban	62	1.124	0.049	1.024

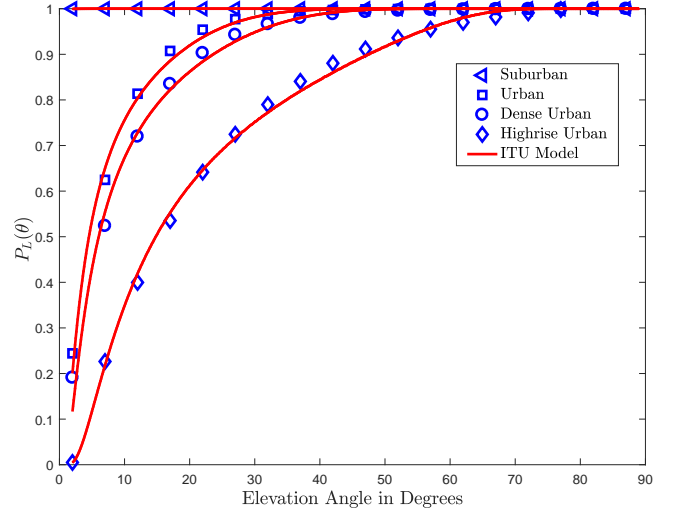


Fig. 2. LoS probability versus the elevation angle for different environments.

Fig. 2 shows the LoS probability using the original ITU model in (1) and the approximated expression in (2) for different environments. It can be seen that the approximated LoS expression in (2) matches the original ITU model very closely. Each C2A link between the aerial user, which is at a height  $h_{UT} = h_U - h_T$  from the terrestrial-BSs, and a terrestrial-BS is assumed to be either a LoS or a NLoS link with a LoS probability  $P_L(z)$  given by

$$P_L(z) = -a \exp \left( -b \tan^{-1} \left( \frac{h_{UT}}{z} \right) \right) + c. \quad (3)$$

Finally, the NLoS probability is given by  $P_N(z) = 1 - P_L(z)$ .

Due to the fact that the aerial user is either in a LoS or a NLoS condition with each terrestrial-BS [22], the set of terrestrial-BSs can be decomposed into two independent inhomogeneous PPPs, where the LoS terrestrial-BSs form a subset  $\Phi_L$  with density  $\lambda_T P_L(z)$  while the NLoS terrestrial-BSs form a subset  $\Phi_N$  with density  $\lambda_T P_N(z)$  [23]. We assume that the LoS and NLoS C2A channels experience Nakagami- $m$  fading with different  $m$  parameters, and therefore the received power from the terrestrial-BS located at point  $x_j$  is Gamma distributed, i.e.,  $H_\nu^{x_j} \sim \text{Gamma} \left( m_\nu, \frac{1}{m_\nu} \right)$  where  $m_\nu$ ,  $\nu \in \{L, N\}$  denotes the fading parameters for the LoS and NLoS C2A links. The probability density function (PDF) of the Gamma-distributed channel gain is given by

$$f_{H_\nu^{x_j}}(x) = \frac{m_\nu^{m_\nu} x^{m_\nu-1}}{\Gamma(m_\nu)} e^{-m_\nu x}, \quad \nu \in \{L, N\}, \quad (4)$$

where  $\Gamma(\cdot)$  is the Gamma function defined as  $\Gamma(m_\nu) = \int_0^\infty t^{m_\nu-1} e^{-t} dt$ . The received power at the typical aerial user

from a BS located at point  $x_j$  is given by

$$P_{r,j}^\nu = P_T \eta_\nu G_{\text{sl}} H_\nu^{x_j} d_{\nu,x_j}^{-\alpha_\nu}, \quad \nu \in \{L, N\}, \quad (5)$$

where  $\eta_\nu$  are the excess losses for the LoS and NLoS C2A links, respectively. Moreover,  $G_{\text{sl}}$  is the sidelobe gain of the terrestrial-BSs antennas since they are usually tilted down towards terrestrial users,  $d_{\nu,x_j}$  denotes the distance between the typical aerial user and a terrestrial-BS from the tier  $\Phi_\nu, \nu \in \{L, N\}$  located at  $x_j$ . Finally,  $\alpha_\nu, \nu \in \{L, N\}$ , is the path-loss coefficient.

### B. Air-to-air channel

Since the aerial user is assumed to hover above rooftops, the A2A links between the typical aerial user and the aerial-BSs are assumed to be in LoS conditions [24], [25]. We assume that the aerial-BSs employ directive beamforming to improve the SINR. Finally, the gain of the aerial-BS antenna, denoted by  $G_r$ , is given by [26]

$$G_r = \begin{cases} G_A, & -\frac{\theta_B}{2} \leq \psi \leq \frac{\theta_B}{2} \\ g_A, & \text{otherwise,} \end{cases} \quad (6)$$

where  $G_A$  and  $g_A$  are the gains of the main lobes and side lobes, respectively,  $\psi$  is the sector angle, and  $\theta_B \in [0, 180]$  is the beamwidth in degrees. The received power at the aerial user from an aerial-BS located at  $x_i$  is given by

$$P_{r,i}^A = P_A G_r \eta_A H_A^{x_i} d_{A,x_i}^{-\alpha_A}, \quad (7)$$

where  $\eta_A$  represents the excess losses,  $H_A^{x_i}$  is the Gamma-distributed channel gain, i.e.,  $H_A^{x_i} \sim \text{Gamma}\left(m_A, \frac{1}{m_A}\right)$ , with a fading parameter  $m_A$ .  $d_{A,x_i}$  denotes the distance between the typical aerial user and the aerial-BS located at  $x_i$ , and  $\alpha_A$  is the path-loss exponent. Unlike terrestrial-BSs whose antennas are downtilted towards terrestrial users, the aerial-BSs can direct their beams towards their associated aerial users. Hence, the beamforming gain from the serving aerial-BS is always  $G_A$  [27]. For the remaining interfering aerial-BSs, their main beams are not necessarily aligned with the typical aerial user. We introduce a probability  $q_A$  depending on the beamwidth  $\theta_B$  that quantifies the likelihood that an interfering aerial-BS's main lobe is directed towards the typical aerial-UE. The interfering aerial-BS gain is  $g_A$  when the typical receiver is in its sidelobe direction with a probability of occurrence of  $1 - q_A$ . Typically,  $g_A$  is 20 dB less than the main lobe gain  $G_A$  [27].

The typical aerial user is assumed to be served by the BS (located at point  $x_0$ ) that provides the the strongest *long-term averaged* received power [28]. Indeed, since the A2A links are LoS, it may occur that a far aerial-BS offers a better SINR than that provided by a closer terrestrial-BS due to the differences between the path-loss parameters. Note that if the aerial user is associated with a specific tier of BSs, i.e.,  $\{\Phi_L, \Phi_N, \Phi_A\}$ , the serving BS would be the nearest BS from that specific tier. Thus, by assuming that the average power of all channels is 1, i.e.,  $\mathbb{E}[H_L^{x_j}] = \mathbb{E}[H_N^{x_j}] = \mathbb{E}[H_A^{x_j}] = 1$  for each  $x_j \in \Phi_T \cup \Phi_A$ , the serving BS is given by

$$x_0 = \arg \max\{\mu_L R_L^{-\alpha_L}, \mu_N R_N^{-\alpha_N}, \mu_A R_A^{-\alpha_A}\}, \quad (8)$$

where  $\mu_\nu = P_T \eta_\nu G_{\text{sl}}, \nu \in \{L, N\}$ ,  $\mu_A = P_A G_A \eta_A$ ,  $R_L = \min_{\forall x_j \in \Phi_L} d_{L,x_j}$ , and  $R_N = \min_{\forall x_j \in \Phi_N} d_{N,x_j}$ , and  $R_A = \min_{\forall x_i \in \Phi_A} d_{A,x_i}$ . As a result, the SINR at the typical aerial user is given by

$$\gamma = \begin{cases} \frac{\mu_L H_L^{x_0} R_L^{-\alpha_L}}{I + \sigma^2}, & \text{if } x_0 \in \Phi_L(\mathcal{E}_L) \\ \frac{\mu_N H_N^{x_0} R_N^{-\alpha_N}}{I + \sigma^2}, & \text{if } x_0 \in \Phi_N(\mathcal{E}_N) \\ \frac{\mu_A H_A^{x_0} R_A^{-\alpha_A}}{I + \sigma^2}, & \text{if } x_0 \in \Phi_A(\mathcal{E}_A), \end{cases} \quad (9)$$

where  $\mathcal{E}_\nu, \nu \in \{L, N, A\}$ , denotes the event that the serving BS belongs to the tier  $\Phi_\nu$  and  $\sigma^2$  is the additive white Gaussian noise power. Finally,  $I$  refers to the aggregate interference power.

Two spectrum sharing policies between the aerial-BSs and terrestrial-BSs are used, i.e., orthogonal spectrum sharing (OSS) and non-orthogonal spectrum sharing (N-OSS) [29]. OSS/N-OSS implies that aerial-BSs and terrestrial-BSs operate on same/different frequencies. The interference  $I$  is given by

$$I = \begin{cases} I_L + I_N + I_A, & \text{N-OSS} \\ I_L + I_N, & \text{OSS, if } x_0 \in \Phi_L \cup \Phi_N \\ I_A, & \text{OSS, if } x_0 \in \Phi_A, \end{cases} \quad (10)$$

where

$$I_L = \sum_{x_j \in \Phi_L \setminus x_0} \mu_L H_L^{x_j} d_{L,x_j}^{-\alpha_L}, \quad I_N = \sum_{x_j \in \Phi_N \setminus x_0} \mu_N H_N^{x_j} d_{N,x_j}^{-\alpha_N},$$

$$\text{and, } I_A = \sum_{i=1, x_i \in \Phi_A \setminus x_0}^N P_A G_r \eta_A H_A^{x_i} d_{A,x_i}^{-\alpha_A}, \quad (11)$$

where  $G_r = G_A$  with a probability of  $q_A$  and  $G_r = g_A$  with a probability of  $1 - q_A$ .

## III. RELEVANT DISTANCE DISTRIBUTIONS AND ASSOCIATION PROBABILITIES

In this section, we first derive several relevant distance distributions which will be useful in deriving the association probabilities and the Laplace transforms of the interference powers given in (10). Finally, simplified expressions for the association probabilities and the terrestrial interference's Laplace transform are presented under the assumption that all the C2A links are in LoS conditions.

### A. Distance distributions of the nearest BSs

In Lemma 1, we present the distribution of the distances between the aerial user and the nearest aerial-BS, LoS terrestrial-BS and NLoS terrestrial-BS.

**Lemma 1.** The PDF and CDF of  $R_\nu, \nu \in \{L, N\}$  are given by

$$f_{R_\nu}(r) = 2\pi\lambda_T r P_\nu \left( \sqrt{r^2 - h_{\text{UT}}^2} \right) \times \exp\left(-2\pi\lambda_T \int_{h_{\text{UT}}}^r t P_\nu \left( \sqrt{t^2 - h_{\text{UT}}^2} \right) dt\right), r \geq h_{\text{UT}} \quad (12)$$

$$F_{R_\nu}(r) = 1 - \exp\left(-2\pi\lambda_T \int_{h_{\text{UT}}}^r t P_\nu \left( \sqrt{t^2 - h_{\text{UT}}^2} \right) dt\right), r \geq h_{\text{UT}} \quad (13)$$

*Proof:* See Appendix A.

The PDF and the CDF of  $R_A$  are given by [14, eq. (7)]

$$f_{R_A}(r) = N \left( \frac{2r}{r_D^2} \right) \left( \frac{d^2 - r^2}{r_D^2} \right)^{N-1}, h_{UA} \leq r \leq d \quad (14)$$

$$F_{R_A}(r) = \begin{cases} 0, & r \leq h_{UA} \\ 1 - \left( \frac{d^2 - r^2}{r_D^2} \right)^N, & h_{UA} \leq r \leq d \\ 1, & r \geq d, \end{cases} \quad (15)$$

where  $d = \sqrt{r_D^2 + h_{UA}^2}$ .

### B. Distances of the nearest interfering BSs

In Table II, we summarize the distances  $\tau_{\nu|\mathcal{E}_\nu}(r), \nu \in \{L, N, A\}$  between the typical aerial user and the nearest interfering BSs from the three tiers  $\Phi_L, \Phi_N, \Phi_A$  given that the serving BS is at a distance  $r$ . Note that  $N'$  in Table II quantifies the number of interfering aerial-BSs.

### C. Association probabilities

As stated previously, the aerial user is associated with an aerial-BS, LoS terrestrial-BS, or NLoS terrestrial-BS with probabilities given in the following lemmas.

**Lemma 2.** The probability that the typical aerial user is associated with a LoS terrestrial-BS is given by

$$\mathcal{A}_L = \Xi_L^L \times \Xi_A^L, \quad (16)$$

where

$$\Xi_N^L = \begin{cases} F_{R_L}(\zeta_N^L) + \int_{\zeta_N^L}^{\infty} F_{R_N}^{(c)} \left( \left( \frac{\eta_N r^{\alpha_L}}{\eta_L} \right)^{\frac{1}{\alpha_N}} \right) f_{R_L}(r) dr, & h_{UT} \leq \zeta_N^L \\ \int_{\zeta_N^L}^{\infty} F_{R_N}^{(c)} \left( \left( \frac{\eta_N r^{\alpha_L}}{\eta_L} \right)^{\frac{1}{\alpha_N}} \right) f_{R_L}(r) dr, & h_{UT} \geq \zeta_N^L, \end{cases} \quad (17)$$

and,

$$\Xi_A^L = \begin{cases} 1 + \int_{\zeta}^{\zeta_A^L(d)} F_{R_A}^{(c)} \left( \left( \frac{\mu_A r^{\alpha_A}}{\mu_L} \right)^{\frac{1}{\alpha_A}} \right) f_{R_L}(r) dr - F_{R_L}^{(c)}(\zeta), & h_{UT} \leq \zeta_A^L(d) \\ 0, & h_{UT} \geq \zeta_A^L(d), \end{cases} \quad (18)$$

with  $\zeta = \arg \max \{h_{UT}, \zeta_A^L(h_{UA})\}$ .

*Proof:* See Appendix B.

**Lemma 3.** The probability that the typical aerial user is associated with an aerial-BS is given by

$$\mathcal{A}_A = \Xi_N^A \times \Xi_L^A, \quad (19)$$

where

$$\Xi_N^A = \begin{cases} \int_{h_{UA}}^d F_{R_N}^{(c)} \left( \left( \frac{\mu_N r^{\alpha_A}}{\mu_A} \right)^{\frac{1}{\alpha_N}} \right) f_{R_A}(r) dr, & \zeta_N^A \leq h_{UA} \\ F_{R_A}(\zeta_N^A) + \int_{\zeta_N^A}^d F_{R_N}^{(c)} \left( \left( \frac{\mu_N r^{\alpha_A}}{\mu_A} \right)^{\frac{1}{\alpha_N}} \right) f_{R_A}(r) dr, & h_{UA} \leq \zeta_N^A \leq d \\ 1, & \zeta_N^A \geq d, \end{cases} \quad (20)$$

where  $\zeta_N^A = \left( \frac{\mu_A h_{UT}^{\alpha_N}}{\mu_N} \right)^{\frac{1}{\alpha_A}}$ , and,

$$\Xi_L^A = \begin{cases} \int_{h_{UA}}^d F_{R_L}^{(c)} \left( \left( \frac{\mu_L r^{\alpha_A}}{\mu_A} \right)^{\frac{1}{\alpha_L}} \right) f_{R_A}(r) dr, & \zeta_L^A \leq h_{UA} \\ F_{R_A}(\zeta_L^A) + \int_{\zeta_L^A}^d F_{R_L}^{(c)} \left( \left( \frac{\mu_L r^{\alpha_A}}{\mu_A} \right)^{\frac{1}{\alpha_L}} \right) f_{R_A}(r) dr, & h_{UA} \leq \zeta_L^A \leq d \\ 1, & \zeta_L^A \geq d. \end{cases} \quad (21)$$

*Proof:* The proof follows the same steps as that of Lemma 2, therefore omitted here.

Finally, the probability that the aerial user is associated with a NLoS terrestrial-BS is given by  $\mathcal{A}_N = 1 - \mathcal{A}_L - \mathcal{A}_A$ .

### D. Conditional distance distributions of the serving BS

In this section, we present the distribution of the distances between the aerial user and the serving-BS given that it is associated with an aerial-BS, LoS terrestrial-BS or NLoS terrestrial-BS.

**Lemma 4.** Given that the aerial user is associated with a LoS terrestrial-BS (i.e., the event  $\mathcal{E}_L$  occurs), the distribution of the distance  $\tilde{R}_L$  between the aerial user and the serving LoS terrestrial-BS is given by

$$f_{\tilde{R}_L|\mathcal{E}_L}(r) = \begin{cases} \frac{1}{\mathcal{A}_L} F_{R_N}^{(c)}(\tau_{N|\mathcal{E}_L}(r)) \times F_{R_A}^{(c)}(\tau_{A|\mathcal{E}_L}(r)) \times f_{R_L}(r), & r \in \mathfrak{R}_L \\ 0, & \text{otherwise,} \end{cases} \quad (22)$$

where  $\mathfrak{R}_L = [h_{UT}, \zeta_A^L(d)]$ . Note that according to (18),  $\mathcal{A}_L = 0$  outside  $\mathfrak{R}_L$ .

*Proof:* See Appendix C.

**Lemma 5.** Given that the aerial user is associated with an aerial-BS (i.e., the event  $\mathcal{E}_A$  occurs), the distribution of the distance  $\tilde{R}_A$  between the aerial user and the serving aerial-BS is given by

$$f_{\tilde{R}_A|\mathcal{E}_A}(r) = \begin{cases} \frac{1}{\mathcal{A}_A} F_{R_N}^{(c)}(h_{UT}) \times F_{R_L}^{(c)}(\tau_{L|\mathcal{E}_A}(r)) \times f_{R_A}(r), & r \in \mathfrak{R}_A \\ 0, & \text{otherwise,} \end{cases} \quad (23)$$

where  $\mathfrak{R}_A = [h_{UA}, d]$ .

*Proof:* The proof follows the same steps as that of Lemma 4, therefore omitted here.

**Lemma 6.** Given that the aerial user is associated with a NLoS terrestrial-BS (i.e., the event  $\mathcal{E}_N$  occurs), the distribution of the distance  $\tilde{R}_N$  between the aerial user and the serving NLoS terrestrial-BS is given by

$$f_{\tilde{R}_N|\mathcal{E}_N}(r) = \begin{cases} \frac{1}{\mathcal{A}_N} F_{R_L}^{(c)}(\tau_{L|\mathcal{E}_N}(r)) \times F_{R_A}^{(c)}(h_{UA}) \times f_{R_N}(r), & r \in \mathfrak{R}_N \\ 0, & \text{otherwise,} \end{cases} \quad (24)$$

where  $\mathfrak{R}_N = [h_{UT}, d]$ .

TABLE II  
INTERFERERS DISTANCES

Condition	$\tau_{L \mathcal{E}_\nu}(r)$	$\tau_{N \mathcal{E}_\nu}(r)$	$\tau_{A \mathcal{E}_\nu}(r)$	$N'$
$\mathcal{E}_L (x_0 \in \Phi_L)$	$r$	$\begin{cases} h_{UT}, & h_{UT} \leq r \leq \zeta_N^L \\ \left(\frac{\eta_N r^{\alpha_N}}{\eta_L}\right)^{\frac{1}{\alpha_N}}, & r \geq \zeta_N^L, \end{cases}$ where $\zeta_N^L = \left(\frac{\eta_L h_{UT}^{\alpha_N}}{\eta_N}\right)^{\frac{1}{\alpha_L}}$	$\begin{cases} h_{UA}, & h_{UT} \leq \zeta_A^L(h_{UA}) \\ \left(\frac{\mu_A r^{\alpha_A}}{\mu_L}\right)^{\frac{1}{\alpha_A}}, & \zeta_A^L(h_{UA}) \leq r \leq \zeta_A^L(d), \end{cases}$ where $\zeta_A^L(x) = \left(\frac{\mu_L x^{\alpha_A}}{\mu_A}\right)^{\frac{1}{\alpha_L}}$	N
$\mathcal{E}_N (x_0 \in \Phi_N)$	$\left(\frac{\mu_L r^{\alpha_N}}{\mu_N}\right)^{\frac{1}{\alpha_L}}$	$r$	$h_{UA}$	N
$\mathcal{E}_A (x_0 \in \Phi_A)$	$\begin{cases} h_{UT}, & h_{UA} \leq r \leq \zeta_L^A \\ \left(\frac{\mu_L r^{\alpha_A}}{\mu_A}\right)^{\frac{1}{\alpha_L}}, & \zeta_L^A \leq r \leq d. \end{cases}$ where $\zeta_L^A = \left(\frac{\mu_A h_{UT}^{\alpha_A}}{\mu_L}\right)^{\frac{1}{\alpha_A}}$	$h_{UT}$	$r$	N-1

### E. Laplace transform of the aggregated interference

Depending on the spectrum sharing policy, the aerial user may receive interference signals from aerial-BSs and terrestrial-BSs whose Laplace transforms are characterized in the following lemmas.

**Lemma 7.** Conditioned on the event  $\mathcal{E}_\nu$ ,  $\nu \in \{L, N, A\}$ , the Laplace transform of the terrestrial interference power,  $I_L + I_N$ , is given by

$$\mathcal{L}_{(I_N+I_L)|\mathcal{E}_\nu}(s) = \prod_{\omega \in \{L, N\}} \exp\left(-2\pi\lambda_T \int_{\tau_{\omega|\mathcal{E}_\nu}(r)}^{\infty} \left(1 - \left(\frac{m_\omega}{m_\omega + s\mu_\omega t^{-\alpha_\omega}}\right)^{m_\omega}\right) t P_\omega\left(\sqrt{t^2 - h_{UT}^2}\right) dt\right). \quad (25)$$

*Proof:* See Appendix D.

**Lemma 8.** Conditioned on the event  $\mathcal{E}_\nu$ ,  $\nu \in \{L, N, A\}$ , the Laplace transform of the aerial interference power,  $I_A$ , is given by

$$\begin{aligned} \mathcal{L}_{I_A|\mathcal{E}_\nu}(s) &= \sum_{i=0}^{N'} \binom{N'}{i} \left(\frac{2m_A^{m_A} (sP_A\eta_A)^{-m_A}}{\alpha_A \Gamma(m_A)(d^2 - r^2)}\right)^{N'} \\ &\times [q_A (\Omega(d, G_A) - \Omega(\tau_{A|\mathcal{E}_\nu}(r), G_A))]^{N'-i} \\ &\times [(1 - q_A) (\Omega(d, g_A) - \Omega(\tau_{A|\mathcal{E}_\nu}(r), g_A))]^i, \end{aligned} \quad (26)$$

where  $\Omega[\cdot, \cdot]$  is given below by

$$\Omega(x, g) = \frac{x^{\alpha_A m_A + 2}}{g^{m_A}} G_{2,2}^{1,2} \left[ \begin{matrix} m_A x^{\alpha_A} \\ sP_A g \eta_A \end{matrix} \middle| \begin{matrix} 1 - m_A - \frac{2}{\alpha_A}, 1 - m_A \\ 0, -m_A - \frac{2}{\alpha_A} \end{matrix} \right], \quad (27)$$

where  $G[\cdot]$  is the Meijer-G function given in [30, eq. (9.301)].

*Proof:* See Appendix E.

### F. Simplified C2A channel model

The previous results (association probabilities and Laplace transform of interference) require numerical evaluations of multiple integrals. These expressions can be simplified by noting that the aerial user may hover at high heights resulting in LoS transmissions with the terrestrial-BSs. Therefore, we assume that the C2A links are in LoS conditions with the aerial user. The validity of this assumption will be investigated with

simulations in Section V. Under this assumption, the PDF and CDF of the distance between the aerial user and the nearest LoS terrestrial-BS are given by [27, eqs. (8) and (9)]

$$f_{R_L}(r) = 2\pi\lambda_T r \exp(-\pi\lambda_T (r^2 - h_{UT}^2)), \quad r \geq h_{UT} \quad (28)$$

$$F_{R_L}(r) = 1 - \exp(-\pi\lambda_T (r^2 - h_{UT}^2)), \quad r \geq h_{UT}. \quad (29)$$

**Corollary 1.** With the assumption that the aerial user experience LoS conditions with the terrestrial-BSs, the association probability to a terrestrial-BS given in (16) can be written as in (30) at the top of the next page, where  $\Upsilon(x) = \Gamma\left[\frac{\alpha_A}{\alpha_A} i + 1, \pi\lambda_T x^2\right]$ , with  $\Gamma[\cdot, \cdot]$  denoting the upper incomplete Gamma function [30, eq. (8.358.2)]. Thus, the probability of association to an aerial-BS is given by  $\mathcal{A}_A = 1 - \mathcal{A}_L$ .

*Proof:* Substitute (28) into (18) and apply the Binomial theorem. Then, using the definition of the upper incomplete Gamma function and with some manipulations, we obtain (30).

**Corollary 2.** The Laplace transform of the terrestrial interference,  $\mathcal{L}_{I_L|\mathcal{E}_\nu}(s)$ , where  $\nu \in \{L, A\}$ , is given by

$$\begin{aligned} \mathcal{L}_{I_L|\mathcal{E}_\nu}(s) &= \exp\left(-2\pi\lambda_T \sum_{i=0}^{m_L-1} \left(\frac{s\mu_L}{m_L}\right)^{1+i-m_L} \frac{1}{\alpha_L \Gamma[m_L - i]}\right. \\ &\left. \times \tau_{L|\mathcal{E}_\nu}(r)^{\alpha_L(m_L - i - 1)} \Theta(s, \tau_{L|\mathcal{E}_\nu}(r))\right), \end{aligned} \quad (31)$$

where  $\Theta(\cdot, \cdot)$  is defined as

$$\Theta(s, r) = G_{2,2}^{2,1} \left[ \begin{matrix} m_L r^{\alpha_L} \\ s\mu_L \end{matrix} \middle| \begin{matrix} 1+i-m_L, 2+i-m_L - \frac{2}{\alpha_L} \\ 1+i-m_L - \frac{2}{\alpha_L}, 0 \end{matrix} \right]. \quad (32)$$

*Proof:* Starting from (25), substituting  $P_L(t) = 1$ ,  $t \geq h_{UT}$  and applying the identity  $a^n - b^n = (a - b) \sum_{i=0}^{n-1} a^i b^{n-1-i}$ , [31, eq. (1.43)], and [30, eq. (7.811.2)] yield (31).

## IV. COVERAGE AND RATE ANALYSIS

### A. Downlink coverage probability

The coverage probability is defined as the probability that the SINR at the typical aerial user exceeds a predetermined

$$A_L = \begin{cases} 1 - \exp(-\pi\lambda_T(\zeta^2 - h_{UT}^2)) + \frac{\pi\lambda_T h_{UT}^2}{r_D^2 N} \sum_{i=0}^N \binom{N}{i} (-1)^i d^{2(N-i)} \left(\frac{\mu_A}{\mu_L}\right)^{\frac{2i}{\alpha_A}} (\pi\lambda_T)^{-\frac{\alpha_L i}{\alpha_A}} \\ \times [\Upsilon(\zeta) - \Upsilon(\zeta_A^L(d))], \\ 0, \end{cases} \quad \begin{aligned} h_{UT} &\leq \zeta_A^L(d) \\ h_{UT} &\geq \zeta_A^L(d). \end{aligned} \quad (30)$$

threshold  $T$ . By applying the law of total probability, the coverage probability at the typical aerial user is given by

$$C = \sum_{\nu \in \{L, N, A\}} A_\nu \times C_\nu, \quad (33)$$

where  $A_\nu$  and  $C_\nu$ ,  $\nu \in \{L, N, A\}$  denote the the association probability to the  $\Phi_\nu$  tier and the coverage probability given that the aerial user is associated with the BS from  $\Phi_\nu$ , respectively.

**Theorem 1.** *The coverage probability  $C_\nu$  conditioned on the events  $\mathcal{E}_\nu$ ,  $\nu \in \{L, N, A\}$  is given by*

$$C_\nu = \sum_{k=0}^{m_\nu-1} \frac{(-1)^k}{k!} \left(\frac{m_\nu T}{\mu_\nu}\right)^k \int_{r \in \mathfrak{R}_\nu} r^{k\alpha_\nu} \left[ \frac{\partial^k}{\partial s^k} \mathcal{L}_{V|\mathcal{E}_\nu}(s) \right]_{s=\frac{m_\nu T r^{\alpha_\nu}}{\mu_\nu}} f_{\tilde{R}_\nu|\mathcal{E}_\nu}(r) dr, \quad (34)$$

where  $V = I + \sigma^2$  and  $\mathcal{L}_{V|\mathcal{E}_\nu}(s)$  is given by  $\mathcal{L}_{V|\mathcal{E}_\nu}(s) = \exp(-\sigma^2 s) \mathcal{L}_{I|\mathcal{E}_\nu}(s)$ .

Note that under N-OSS policy,  $\mathcal{L}_{I|\mathcal{E}_\nu}(s) = \mathcal{L}_{(I_N + I_L)|\mathcal{E}_\nu}(s) \times \mathcal{L}_{I_A|\mathcal{E}_\nu}(s)$ .

*Proof:* See Appendix F.

### B. Downlink average achievable rate

In this section, we derive the average achievable rate of the typical aerial user. Following the same analysis as the coverage probability, the average ergodic rate is given by

$$\mathcal{R} = \sum_{\nu \in \{L, N, A\}} A_\nu \times \mathcal{R}_\nu, \quad (35)$$

where  $\mathcal{R}_\nu$  is the average achievable rate of the aerial user when it is associated with a BS from the tier  $\Phi_\nu$ .

**Theorem 2.** *The average achievable rate of the typical aerial user given that it is associated with  $\Phi_\nu$  tier is given by*

$$\mathcal{R}_\nu = \sum_{k=0}^{m_\nu-1} \frac{(-1)^k}{\ln(2)k!} \left(\frac{m_\nu}{\mu_\nu}\right)^k \int_0^\infty \int_{r \in \mathfrak{R}_\nu} r^{k\alpha_\nu} (e^t - 1)^k \left[ \frac{\partial^k}{\partial s^k} \mathcal{L}_{V|\mathcal{E}_\nu}(s) \right]_{s=\frac{m_\nu(e^t-1)r^{\alpha_\nu}}{\mu_\nu}} f_{\tilde{R}_\nu|\mathcal{E}_\nu}(r) dr dt, \quad (36)$$

*Proof:* Using Shannon's theorem, the average achievable rate can be expressed as

$$\mathcal{R}_\nu = \frac{1}{\ln(2)} \mathbb{E}_{\tilde{R}_\nu} [\mathbb{E}_\gamma [\ln(1 + \gamma)]] \\ \stackrel{(a)}{=} \frac{1}{\ln(2)} \mathbb{E}_{\tilde{R}_\nu} \left[ \int_0^\infty \mathbb{P}(\gamma \geq e^t - 1) dt \right], \quad (37)$$

where (a) follows from  $\mathbb{E}[Z] = \int_0^\infty \mathbb{P}(Z > t) dt$ . Substituting (9) into (37) and following the same steps as those of Theorem 1 yields (36).

TABLE III  
PARAMETERS VALUES

Parameter	value	Parameter	value
$(P_T, P_A)$	(43, 30) dBm	$(m_L, m_N, m_A)$	(2,1,2)
$r_D$	2000 meters	N	10
$G_{sl}$	-15 dB	$(\eta_L, \eta_N, \eta_A)$	(-3, -20, -1) dB
$(\alpha_L, \alpha_N, \alpha_A)$	(2.5, 3.5, 2)	$\sigma^2$	-113 dBm
$\lambda_T$	5	$T$	5 dB
Policy	N-OSS	Environment	Urban
$q_A$	0.1	$(h_U, h_A)$	(50,300) meters

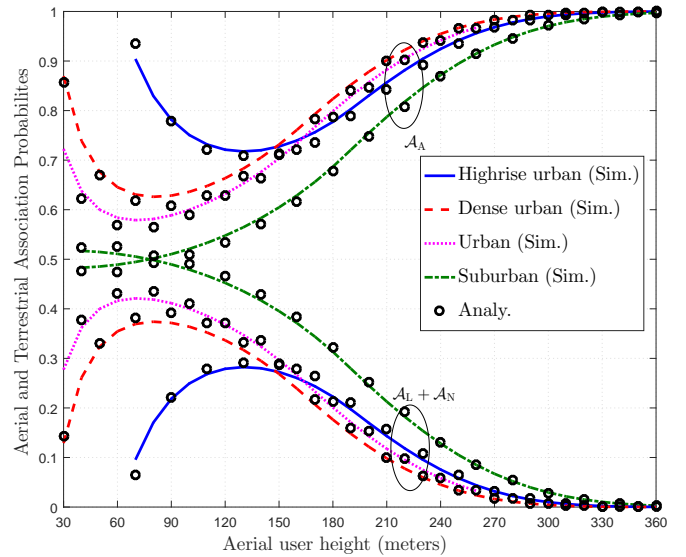


Fig. 3. Association probability versus the aerial user height with  $h_A = 500$  meters.

## V. RESULTS AND DISCUSSIONS

In this section, we use Monte Carlo simulations to validate the analytical expressions. We also investigate the impact of several system parameters on the network performance. Table III summarizes the parameters used in the simulations unless referred otherwise.

We compare aerial-BS and terrestrial-BS association probabilities with different heights of the aerial user and environments in Fig. 3. At low heights of the aerial user, this latter tends to be associated with an aerial-BS because the C2A links are dominated by NLoS links which have poor channel conditions in comparison to the LoS A2A links. As the height increases, the terrestrial-BS association probability increases since more terrestrial-BSs are in LoS conditions with the aerial user. However, with a further increase in the height, the terrestrial-BS association probability starts to decrease because of the large path-losses caused by the large distances between the aerial user and the terrestrial-BSs.

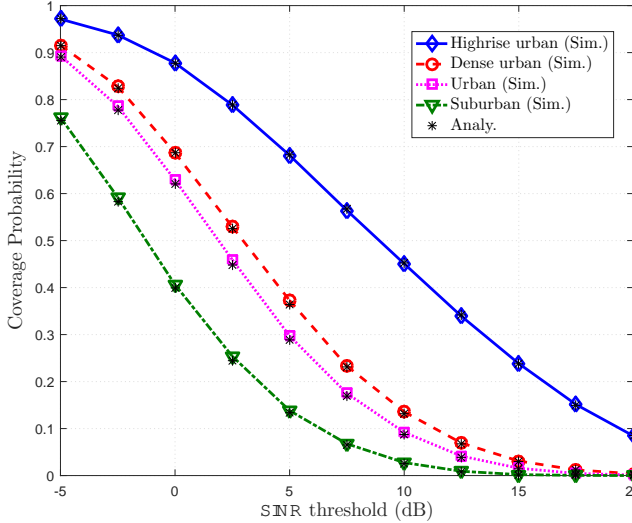


Fig. 4. Coverage probability versus SINR threshold:  $h_U = 70$  meters and  $h_A = 200$  meters.

Fig. 4 shows the coverage probability versus the SINR threshold for different environments. For a particular SINR threshold and as the environment becomes less dense, more terrestrial-BSs are in LoS conditions with the aerial user (i.e., more interfering LoS terrestrial-BSs) which increases the interference.

In Fig. 5, we compare the coverage probability with different heights of the aerial user under OSS and N-OSS policies. Under N-OSS policy, as the aerial user height increases, more terrestrial-BSs are in LoS conditions with the aerial user which increases the terrestrial interference at a larger rate than the increase in the desired signal power. For the OSS policy, a different trend can be observed at low heights of the aerial user, i.e., the coverage probability increases. This is because at very low heights of the aerial user, the improvement in the desired signal power is larger than the increase in the terrestrial interference (since the aerial user may experience LoS conditions with few terrestrial-BSs while terrestrial interference is dominated by NLoS terrestrial-BSs). However, with a further increase in the aerial user height, the interference received from the LoS terrestrial-BSs dominates which degrades the coverage probability. It can also be seen that under the assumption that the C2A links are all LoS links, the coverage probability converges to the actual coverage probability (see Fig. 11(a)).

Fig. 6 shows the coverage probability versus the density of the terrestrial-BSs for different aerial user heights and beamwidths under the OSS and N-OSS policies. Under the N-OSS policy, it can be noticed that the coverage probability decreases as the density of terrestrial-BSs increases due to the increase in the terrestrial interference (more LoS terrestrial-BSs exist as the aerial user height increases). It can also be observed that for a given density of terrestrial-BSs and regardless of the  $q_A$ , the coverage probability decreases as the aerial user height increases due to the increase in the terrestrial interference (terrestrial interference is dominated by LoS terrestrial-BSs). On the other hand, under the OSS policy

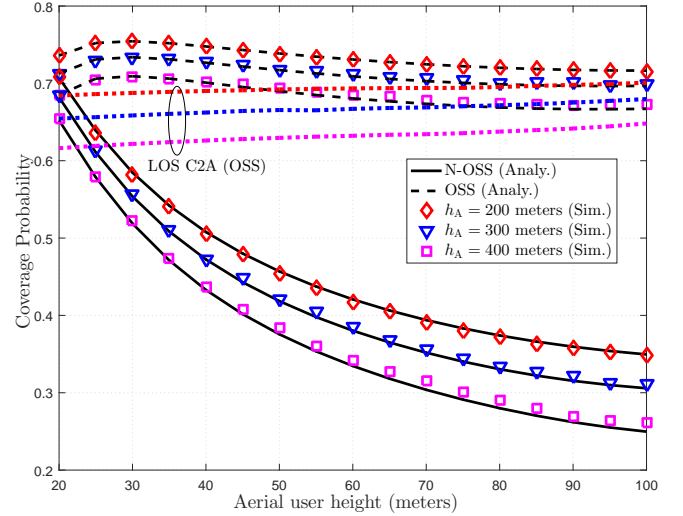


Fig. 5. Coverage probability versus the aerial user height.

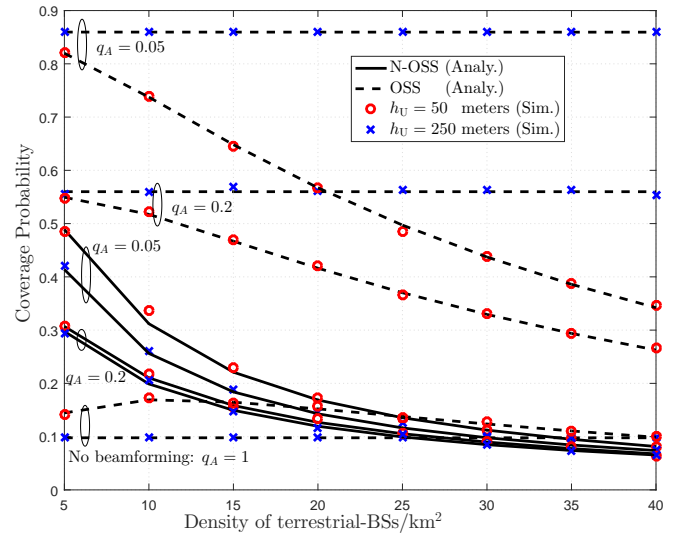


Fig. 6. Coverage probability versus the terrestrial network's density ( $h_A = 300$  meters).

and at a high aerial user height (250 meters), the density of the terrestrial-BSs has no impact on the coverage probability since the aerial user is always associated with an aerial-BS (see Fig. 11(b)) and so it does not receive terrestrial interference. However, a similar trend is not observed if the aerial user is close to the terrestrial-BSs. For instance, at a low aerial user height (50 meters), the coverage probability decreases as the density of the terrestrial-BS increases since the aerial user may be associated with a terrestrial-BS and hence increasing the density of terrestrial-BSs increases the terrestrial interference. Overall, aerial BSs with more directed beams (smaller beamwidth implies smaller  $q_A$ ) improves the coverage probability because it decreases the aerial interference power.

We plot the coverage probability versus the number of the aerial-BSs for different heights of the aerial user in Fig. 7. Generally, increasing the number of aerial-BSs decreases the coverage probability due to the fact that the increase in the aerial interference is larger than the increase in the



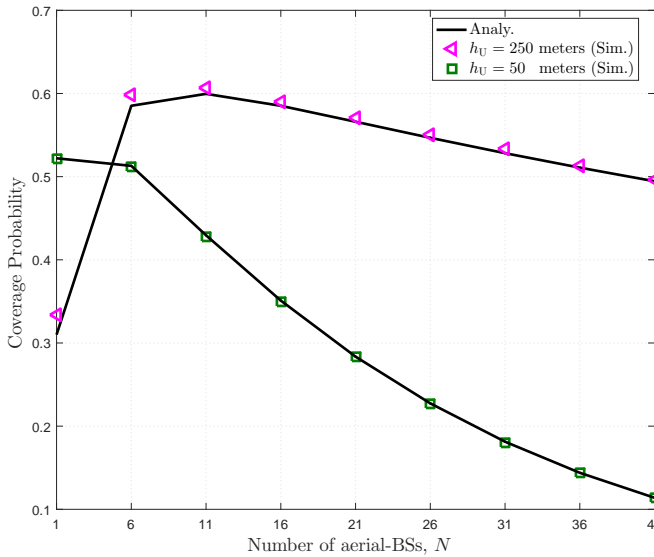


Fig. 7. Coverage probability versus the number of aerial-BSs.

desired signal. However, at high heights of the aerial user (e.g., 250 meters) and low number of aerial-BSs, the coverage probability increases as the number of aerial BSs increases because of the low increase in the aerial interference power (small number of aerial-BSs) compared to the improvement in the aerial desired signal. Overall, denser aerial-BSs decreases the coverage probability especially at low aerial user height.

The validation of the LoS C2A assumption, which is presented in Section III-F, is investigated in Fig. 8. At low heights of the aerial user (e.g.,  $h_U = 30$  meters), it can be easily observed that the LoS C2A assumption is not a good approximation. This is because of the high likelihood of the presence of obstructions (NLoS links) between the aerial user and the terrestrial-BSs. However, at high heights (e.g.,  $h_U = 270$  meters), the aerial user is very likely to experience LoS conditions with the terrestrial-BSs (no or a few NLoS terrestrial-BSs exist) which justifies the correctness and accuracy of the LoS C2A assumption.

The impact of path-loss exponents on the rate is shown in Fig. 9. First, the analytical expression in (35) and the simulations match very closely which substantiates the accuracy of the proposed analytical framework. As expected, the average rates for equal LoS and aerial path-loss exponents show the same behavior since the path-loss exponent will not bias the association of the aerial user. However, under different path-loss exponents for the LoS and aerial links, higher LoS path-loss exponent guarantees a better average rate at the aerial user. This can be explained by the decrease of the terrestrial interference power where LoS and NLoS interference experience more attenuation which yields a higher SINR and as a result higher rate. Finally, the behavior for ( $\alpha_L = 2.5, \alpha_A = 2$ ) aligns with the coverage probability trend in Fig. 7.

Fig. 10 shows the average rate for different heights of the aerial user and fading parameters. At low heights of the aerial user, the rate decreases as the height of the aerial user increases due to the increase in the terrestrial interference (more LoS

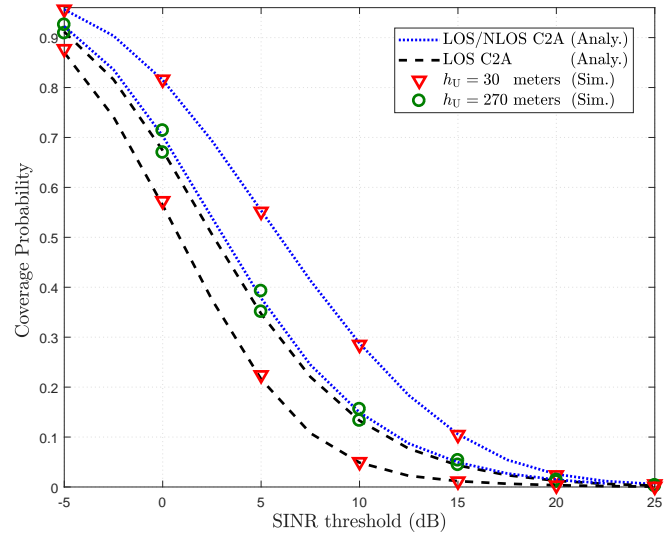


Fig. 8. Coverage probability versus the SINR threshold with  $h_A = 300$  meters.

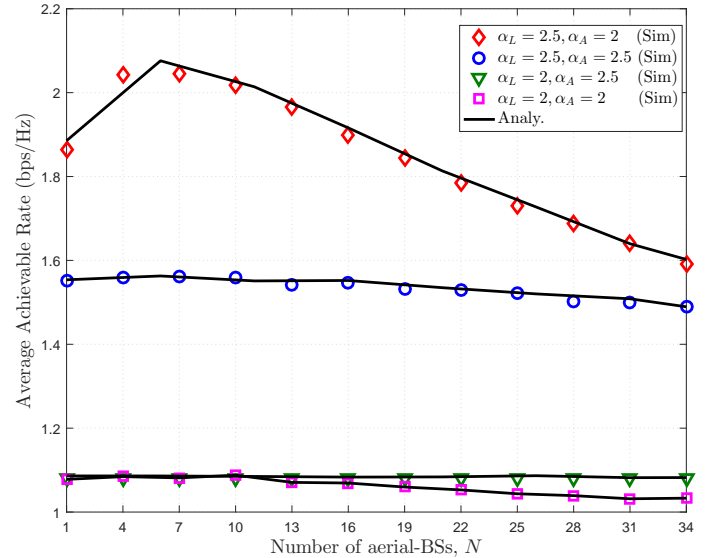


Fig. 9. Average achievable rate versus number of aerial-BSs.

terrestrial-BSs exist). However, with a further increase in the height of the aerial user, the desired signal improves at a higher rate than the terrestrial interference because the C2A links experience high path-losses. Moreover, we observe that the fading parameters do not have a big impact on the rate, especially for no-fading scenario ( $m_A, m_L \rightarrow \infty$ ) where the improvement in the achievable rate does not exceed 0.15 bps/Hz. It can be also observed that the LoS C2A assumption becomes a better approximation to the C2A links as the height of the aerial user increases.

## VI. CONCLUSION

Using stochastic geometry tools, we proposed a framework to analyze coverage probability and rate of a typical aerial user served by a network of aerial-BSs and terrestrial-BSs. Several conclusions can be made from the simulations and the

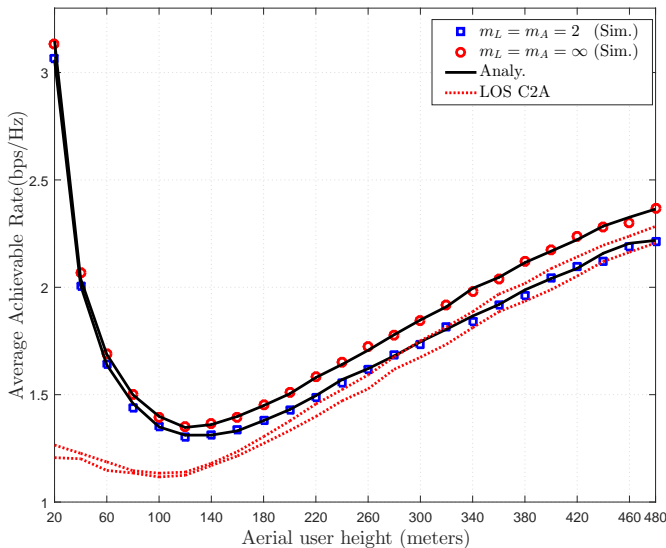
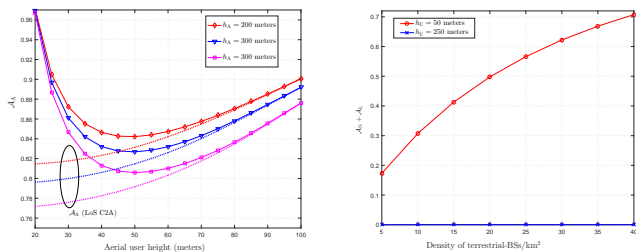


Fig. 10. Average achievable rate versus  $h_U$  ( $h_A = 500$  meters).



(a) Aerial association for Fig. 5. (b) Terrestrial association for Fig. 6.

Fig. 11. Corresponding association probabilities for identified figures.

evaluated analytical expressions. The association probabilities to an aerial-BS and terrestrial-BS depend on the heights of the aerial user and the aerial-BSSs, and the environment. Simulation results show that the aerial user receives strong interference signals from the LoS terrestrial-BSSs and the aerial-BSSs which degrade the coverage probability and rate. The simulations also reveal that the orthogonal spectrum sharing between terrestrial-BSSs and aerial-BSSs improves the coverage probability significantly. Moreover, Directive beamforming reduces the interference received from the LoS aerial-BSSs substantially. Therefore, directive beamforming is essential in the operation of the integrated aerial-terrestrial network. The results also reveal that aerial users of high heights are mainly in LoS conditions with the terrestrial-BSSs (no or a few NLoS links exist). Thus, the analysis can be simplified by assuming two tiers of BSSs (i.e., LoS terrestrial-BSSs and aerial-BSSs). Also, it can be concluded from the results that increasing the density of the aerial-BSSs may or may not degrade the performance depending on the height of both the aerial-BSSs and the aerial user.

#### APPENDIX A PROOF OF LEMMA 1

$R_\nu$  can be written as  $R_\nu = \sqrt{Z_\nu^2 - h_{UT}^2}$ ,  $\nu \in \{L, N\}$ , where  $Z_\nu$  is the horizontal distance between the aerial user

and the nearest LoS and NLoS terrestrial-BSSs. Using the null probability of PPP [32], we have

$$F_{R_\nu}(r) = 1 - \mathbb{P}(R_\nu \geq r) \stackrel{(a)}{=} 1 - \exp\left(-2\pi \int_{h_{UT}}^r \lambda_\Gamma t P_\nu(t) dt\right). \quad (38)$$

Since  $r = \sqrt{z^2 + h_{UT}^2}$ , taking the integral in (a) with respect to  $z$  completes the proof of (13) (note that  $t$  is a dummy variable). (12) can be obtained by differentiating  $F_{R_\nu}(r)$  with respect to  $r$ .

#### APPENDIX B PROOF OF LEMMA 2

The association probability to a LoS terrestrial-BS can be written as

$$\begin{aligned} \mathcal{A}_L &= \mathbb{P}(\mu_L R_L^{-\alpha_L} \geq \mu_N R_N^{-\alpha_N}; \mu_L R_L^{-\alpha_L} \geq \mu_A R_A^{-\alpha_A}) \\ &\stackrel{(a)}{=} \mathbb{P}(\mu_L R_L^{-\alpha_L} \geq \mu_N R_N^{-\alpha_N}) \times \mathbb{P}(\mu_L R_L^{-\alpha_L} \geq \mu_A R_A^{-\alpha_A}) \\ &= \mathbb{P}(R_N \geq \tau_{N|\mathcal{E}_L}(r)) \times \mathbb{P}(R_A \geq \tau_{A|\mathcal{E}_L}(r)) \\ &\stackrel{(b)}{=} \left( \int_{h_{UT}}^{\infty} F_{R_N}^{(c)}(\tau_{N|\mathcal{E}_L}(r)) f_{R_L}(r) dr \right) \\ &\quad \times \left( \int_{h_{UT}}^{\infty} F_{R_A}^{(c)}(\tau_{A|\mathcal{E}_L}(r)) f_{R_L}(r) dr \right), \end{aligned} \quad (39)$$

where (a) follows from the independence of the two point processes that represent the aerial-BSSs and the terrestrial-BSSs, (b) follows from using the definition of the Complementary CDF and averaging over  $R_L$ . Finally, using (13) and (15) along with some mathematical manipulations complete the proof.

#### APPENDIX C PROOF OF LEMMA 3

The CDF of  $\tilde{R}_L$  can be written as

$$\begin{aligned} F_{\tilde{R}_L|\mathcal{E}_L}(r) &= \mathbb{P}[R_L < r | \mathcal{E}_L] \stackrel{(a)}{=} \frac{\mathbb{P}[R_L < r; \mathcal{E}_L]}{\mathbb{P}[\mathcal{E}_L]} \\ &\stackrel{(b)}{=} \frac{\mathbb{P}[R_L \leq r; (R_A \geq \tau_{A|\mathcal{E}_L}(r); R_N \geq \tau_{N|\mathcal{E}_L}(r))]}{\mathcal{A}_L} \\ &= \frac{\mathbb{P}[R_L \leq r; R_A \geq \tau_{A|\mathcal{E}_L}(r)] \mathbb{P}[R_L \leq r; R_N \geq \tau_{N|\mathcal{E}_L}(r)]}{\mathcal{A}_L} \\ &\stackrel{(c)}{=} \frac{1}{\mathcal{A}_L} \int_{h_{UT}}^r F_{R_A}^{(c)}(\tau_{A|\mathcal{E}_L}(r)) F_{R_N}^{(c)}(\tau_{N|\mathcal{E}_L}(r)) f_{R_L}(x) dx, \end{aligned} \quad (41)$$

where (a) follows from Bayes' rule, (b) is obtained from (39), and (c) follows from averaging over  $R_L$ . Finally, differentiating (41) with respect to  $r$  completes the proof.

#### APPENDIX D PROOF OF LEMMA 7

The Laplace transform of the aggregated interference power is given by

$$\begin{aligned} \mathcal{L}_{(I_N + I_L)|\mathcal{E}_\nu}(s) &= \mathbb{E}_{(I_N + I_L)|\mathcal{E}_\nu}[\exp(-s(I_N + I_L))] \\ &\stackrel{(a)}{=} \mathbb{E}_{\Phi_L} \left[ \prod_{x_j \in \Phi_L \setminus x_0} \mathbb{E}_{H_L^{x_j}} \left[ \exp\left(-s \mu_L H_L^{x_j} d_{L,x_j}^{-\alpha_L}\right) \right] \right] \end{aligned}$$

$$\begin{aligned} & \times \mathbb{E}_{\Phi_N} \left[ \prod_{x_j \in \Phi_N \setminus x_0} \mathbb{E}_{H_N^{x_j}} \left[ \exp \left( -s \mu_N H_N^{x_j} d_{N,x_j}^{-\alpha_N} \right) \right] \right] \\ & \stackrel{(b)}{=} \prod_{\omega \in \{L, N\}} \left[ \mathbb{E}_{\Phi_\omega} \left[ \prod_{x_j \in \Phi_\omega \setminus x_0} \left( \frac{m_\omega}{m_\omega + s \mu_\omega d_{\omega,x_j}^{-\alpha_\omega}} \right)^{m_\omega} \right] \right], \end{aligned} \quad (42)$$

where (a) follows from (10) and the independence of the small-scale fading and the PPP, and (b) is obtained from the moment generating function of Gamma distribution. Finally, using the probability generating functional (PGFL) and the results in Table II complete the proof.

#### APPENDIX E PROOF OF LEMMA 8

It was proven in [14, Corollary 3] that given that the serving BS (either terrestrial-BS or aerial-BS) is located at a distance  $r$  from the aerial user, the distribution of the distance between the aerial user and the  $j$ -th interfering aerial-BS  $d_{A,x_j}$ ,  $j \in [1, N']$  is given by

$$f_{d_{A,x_j}}(d_j) = \begin{cases} \frac{2d_j}{d^2 - r^2}, & r \leq d_j \leq d \\ 0, & \text{Otherwise,} \end{cases} \quad (43)$$

where  $N'$  is the number of interfering aerial-BSs. Note that there are  $N' - i$  interfering aerial-BSs that have a gain of  $G_A$  with a probability  $q_A$  and  $i$  interfering aerial-BSs that have a gain of  $g_A$  with probability  $1 - q_A$ . Hence,  $i$  follows a Binomial distribution  $\mathcal{B}(N', q_A)$ . Indeed, the two subsets of interfering BSs (those with gain  $G_A$  and those with gain  $g_A$ ) are dependent where the joint distribution of  $N' - i$  and  $i$  is a multinomial distribution on  $N'$  trials with success probabilities  $q_A$  and  $1 - q_A$ , respectively.

The Laplace transform of the interference received from aerial-BSs is given by

$$\begin{aligned} \mathcal{L}_{I_A | \mathcal{E}_\nu}(s) &= \mathbb{E}_{I_A | \mathcal{E}_\nu} [\exp(-sI_A)] \\ &= \mathbb{E}_{d_{A,x_j}} \left[ \prod_{j=1}^{N'} \mathbb{E}_{H_A^{x_j}} [\exp(-sP_A G_r H_A^{x_j} d_j^{-\alpha_A})] \right] \\ & \stackrel{(a)}{=} \prod_{j=1}^{N'} \left[ \mathbb{E}_{d_{A,x_j}} \left[ \left( \frac{m_A}{m_A + sP_A G_r d_j^{-\alpha_A}} \right)^{m_A} \right] \right] \\ & \stackrel{(b)}{=} f_i(i) \left[ \mathbb{E}_{d_{A,x_j}} \left[ \left( \frac{m_A}{m_A + sP_A G_A d_j^{-\alpha_A}} \right)^{m_A} \right] \right]^{N'-i} \\ & \times \left[ \mathbb{E}_{d_{A,x_j}} \left[ \left( \frac{m_A}{m_A + sP_A g_A d_j^{-\alpha_A}} \right)^{m_A} \right] \right]^i \\ & \stackrel{(c)}{=} \sum_{i=0}^{N'} \binom{N'}{i} q_A^{N'-i} (1 - q_A)^i \\ & \times \left[ \int_{\tau_{A|\mathcal{E}_\nu}(r)}^d \left( \frac{m_A}{m_A + sP_A G_A \eta_A t^{-\alpha_A}} \right)^{m_A} \frac{2t}{d^2 - r^2} dt \right]^{N'-i} \\ & \times \left[ \int_{\tau_{A|\mathcal{E}_\nu}(r)}^d \left( \frac{m_A}{m_A + sP_A g_A \eta_A t^{-\alpha_A}} \right)^{m_A} \frac{2t}{d^2 - r^2} dt \right]^i, \end{aligned} \quad (44)$$

where (a) follows from using the Gamma distribution of the small scale fading channel gain of the A2A link. (b) follows from the binomial distribution of  $i$  with  $f_i(i) = \sum_{i=0}^{N'} \binom{N'}{i} q_A^{N'-i} (1 - q_A)^i$ . (c), is obtained after averaging over  $d_{A,x_j}$ . Using the identity  $(1 + z)^a = 1/\Gamma(-a) G_{1,1}^{1,1}[z | 1^{-a}]$  and [30, eq(7.811.2)] along some additional mathematical manipulations, (26) is obtained.

#### APPENDIX F PROOF OF THEOREM 1

The coverage Probability conditioned to the event that the aerial user is connected to a BS from  $\Phi_\nu$ ,  $\nu \in \{L, N, A\}$ , is given by

$$\begin{aligned} \mathcal{C}_\nu &= \mathbb{P}(\gamma \geq T) \\ & \stackrel{(a)}{=} \mathbb{E}_{H_\nu^{x_0}, \tilde{R}_\nu, I} \left[ \mathbb{P} \left( \frac{\mu_\nu H_\nu^{x_0} r_\nu^{-\alpha_L}}{I + \sigma^2} \geq T \right) \right] \\ & \stackrel{(b)}{=} \mathbb{E}_{\tilde{R}_\nu, V} \left[ \mathbb{E}_{H_\nu^{x_0}} \left[ \mathbb{P} \left( H_\nu^{x_0} \geq \frac{r_\nu^{\alpha_L} T V}{\mu_\nu} \right) \right] \right] \\ & \stackrel{(c)}{=} \mathbb{E}_{\tilde{R}_\nu} \left[ \mathbb{E}_V \left[ \frac{\Gamma \left( m_\nu, \frac{m_\nu T r_\nu^{\alpha_L} V}{\mu_\nu} \right)}{\Gamma(m_\nu)} \right] \right] \\ & \stackrel{(d)}{=} \sum_{k=0}^{m_\nu-1} \frac{1}{k!} \left( \frac{m_\nu T}{\mu_\nu} \right)^k \\ & \times \mathbb{E}_{\tilde{R}_\nu} \left[ r^{k\alpha_\nu} \mathbb{E}_V \left[ V^k \exp \left( \frac{-m_\nu T r^{\alpha_\nu} V}{\mu_\nu} \right) \right] \right], \end{aligned} \quad (45)$$

where (a) follows from averaging the coverage probability over the random variables,  $\{H_\nu^{x_0}, \tilde{R}_\nu, V\}$ , and (b) is obtained by exploiting the independence between the three random variables. Moreover in (45), (c) follows after applying the CCDF of Gamma-distributed channel gain  $H_\nu^{x_0}$  and (d) is obtained by assuming  $m_\nu$  is an integer and using the series expansion of the upper incomplete Gamma function. Finally using the identity, i.e.,  $\mathbb{E}_V [V^k \exp(-sV)] = (-1)^k \frac{\partial \mathcal{L}_V(s)}{\partial s^k}$ , and averaging over  $\tilde{R}_\nu$ , we obtain (34).

#### REFERENCES

- [1] X. Cao, P. Yang, M. Alzenad, X. Xi, D. Wu, and H. Yanikomeroglu, "Airborne communication networks: A survey," *IEEE J. Select. Areas Commun.*, vol. 36, no. 9, pp. 1907–1926, Aug. 2018.
- [2] M. Mozaffari, W. Saad, M. Bennis, Y.-H. Nam, and M. Debbah, "A tutorial on UAVs for wireless networks: Applications, challenges, and open problems," to appear in *IEEE Commun. Surveys Tut.*, 2019, doi: 10.1109/COMST.2019.2902862.
- [3] T. Tomic, K. Schmid, P. Lutz, A. Domel, M. Kassecker, E. Mair, I. L. Grixia, F. Ruess, M. Suppa, and D. Burschka, "Toward a fully autonomous UAV: Research platform for indoor and outdoor urban search and rescue," *IEEE Robotics & Autom. Mag.*, vol. 19, no. 3, pp. 46–56, Sep. 2012.
- [4] S. Hayat, E. Yanmaz, and R. Muzaffar, "Survey on unmanned aerial vehicle networks for civil applications: A communications viewpoint," *IEEE Commun. Surveys Tut.*, vol. 18, no. 4, pp. 2624–2661, Apr. 2016.
- [5] M. Prexl, K. Struebig, J. Harder, and A. Hoehn, "User studies of a head-mounted display for search and rescue teleoperation of UAVs via satellite link," in *Proc. IEEE Aerospace Conf.*, Big Sky, USA, Mar. 2017.
- [6] X. Zhou, J. Guo, S. Durrani, and H. Yanikomeroglu, "Uplink coverage performance of an underlay drone cell for temporary events," in *Proc. IEEE Int. Conf. Commun. (ICC) Workshops*, Kansas City, MO, May 2018, pp. 1–6.

- [7] A. Kumbhar, F. Koochifar, . Gven, and B. Mueller, "A survey on legacy and emerging technologies for public safety communications," *IEEE Commun. Surveys Tut.*, vol. 19, no. 1, pp. 97–124, firstquarter 2017.
- [8] L. Gupta, R. Jain, and G. Vaszkun, "Survey of important issues in UAV communication networks," *IEEE Commun. Surveys Tut.*, vol. 18, no. 2, pp. 1123–1152, secondquarter 2016.
- [9] F. Lagum, I. Bor-Yaliniz, and H. Yanikomeroglu, "Strategic densification with UAV-BSs in cellular networks," *IEEE Wireless Commun. Lett.*, vol. 7, no. 3, pp. 384–387, June 2018.
- [10] A. M. Hayajneh, S. A. R. Zaidi, D. C. McLernon, M. Di Renzo, and M. Ghogho, "Performance analysis of UAV enabled disaster recovery networks: A stochastic geometric framework based on cluster processes," *IEEE Access*, vol. 6, pp. 26 215–26 230, May 2018.
- [11] M. Alzenad and H. Yanikomeroglu, "Coverage and rate analysis for vertical heterogeneous networks (VHetNets)," [Online]. Available: [www.researchgate.net](http://www.researchgate.net). doi: 10.13140/RG.2.2.33855.76964.
- [12] M. M. Azari, F. Rosas, A. Chiumento, and S. Pollin, "Coexistence of terrestrial and aerial users in cellular networks," in *Proc. IEEE Glob. Commun. Conf. (Globecom) Workshops*, Singapore, Dec. 2017.
- [13] M. M. Azari, F. Rosas, and S. Pollin, "Cellular connectivity for UAVs: Network modeling, performance analysis and design guidelines," to appear in *IEEE Trans. Wireless Commun.*, 2019, doi 10.1109/TWC.2019.2910112.
- [14] V. V. Chetlur and H. S. Dhillon, "Downlink coverage analysis for a finite 3-D wireless network of unmanned aerial vehicles," *IEEE Trans. Commun.*, vol. 65, no. 10, pp. 4543–4558, Oct. 2017.
- [15] V. Yajnanarayana, Y. . E. Wang, S. Gao, S. Muruganathan, and X. L. Ericsson, "Interference mitigation methods for unmanned aerial vehicles served by cellular networks," in *2018 IEEE 5G World Forum (5GWF)*, Jul. 2018, pp. 118–122.
- [16] R. Amer, W. Saad, H. ElSawy, M. Butt, and N. Marchetti, "Caching to the sky: Performance analysis of cache-assisted CoMP for cellular-connected UAVs," *arXiv preprint arXiv:1811.11098*, 2018.
- [17] ITU-R, "Recommendation p.1410-5: Propagation data and prediction methods required for the design of terrestrial broadband radio access systems operating in a frequency range from 3 to 60 GHz," *Tech. Rep.*, 2012.
- [18] A. Al-Hourani, S. Kandeepan, and A. Jamalipour, "Modeling air-to-ground path loss for low altitude platforms in urban environments," in *Proc. IEEE Glob. Commun. Conf. (Globecom)*, Austin, TX, USA, Dec. 2014, pp. 2898–2904.
- [19] A. Al-Hourani, S. Kandeepan, and S. Lardner, "Optimal LAP altitude for maximum coverage," *IEEE Wireless Commun. Lett.*, vol. 3, no. 6, pp. 569–572, Dec. 2014.
- [20] D. S. Baum, J. Hansen, J. Salo, G. Del Galdo, M. Milojevic, and P. Kyösti, "An interim channel model for beyond-3G systems: extending the 3GPP spatial channel model (SCM)," in *Proc. IEEE Veh. Technol. Conf.*, vol. 5, Stockholm, Sweden, 2005, pp. 3132–3136.
- [21] J. Holis and P. Pechac, "Elevation dependent shadowing model for mobile communications via high altitude platforms in built-up areas," *IEEE Trans. Anten. Propag.*, vol. 56, no. 4, pp. 1078–1084, Apr. 2008.
- [22] M. Alzenad and H. Yanikomeroglu, "Coverage and rate analysis for unmanned aerial vehicle base stations with LoS/NLoS propagation," in *Proc. IEEE Glob. Commun. Conf. (Globecom) Workshops*, Abu Dhabi, UAE, Dec. 2018, pp. 1–7.
- [23] M. Haenggi, *Stochastic Geometry for Wireless Networks*. Cambridge University Press, 2012.
- [24] M. Walter, S. Gligorević, T. Detert, and M. Schnell, "UHF/VHF air-to-air propagation measurements," in *Proc. fourth European Conf. Ant. Propag.* Silicon Valley, USA: IEEE, 2010, pp. 1–5.
- [25] N. Goddemeier and C. Wietfeld, "Investigation of air-to-air channel characteristics and a UAV specific extension to the rice model," in *Proc. IEEE Glob. Commun. Conf. (Globecom) Workshops*, San Diego, USA, 2015, pp. 1–5.
- [26] M. Mozaffari, W. Saad, M. Bennis, and M. Debbah, "Efficient deployment of multiple unmanned aerial vehicles for optimal wireless coverage," *IEEE Commun. Lett.*, vol. 20, no. 8, pp. 1647–1650, Aug. 2016.
- [27] V. V. Chetlur and H. S. Dhillon, "Coverage and rate analysis of downlink cellular vehicle-to-everything (C-V2X) communication," 2019. [Online]. Available: <http://arxiv.org/abs/1901.09236>
- [28] H. Jo, Y. J. Sang, P. Xia, and J. G. Andrews, "Heterogeneous cellular networks with flexible cell association: A comprehensive downlink SINR analysis," *IEEE Trans. Wireless. Commun.*, vol. 11, no. 10, pp. 3484–3495, Oct. 2012.
- [29] X. Zhou, S. Durrani, J. Guo, and H. Yanikomeroglu, "Underlay drone cell for temporary events: Impact of drone height and aerial channel environments," *IEEE Internet Things J.*, pp. 1–1, 2019.
- [30] I. Gradshteyn and I. Ryzhik, *Table of Integrals, Series, and Products*. Academic Press, Inc., Boston, MA, 1994.
- [31] A. M. Mathai, R. K. Saxena, and H. J. Haubold, *The H-function: Theory and Applications*. Springer Science & Business Media, 2009.
- [32] J. G. Andrews, F. Baccelli, and R. K. Ganti, "A tractable approach to coverage and rate in cellular networks," *IEEE Trans. Commun.*, vol. 59, no. 11, pp. 3122–3134, Nov. 2011.